



THE UNIVERSITY *of* EDINBURGH

Edinburgh Research Explorer

Repeat Subglacial Lake Drainage and Filling beneath Thwaites Glacier

Citation for published version:

Malczyk, G, Gourmelen, N, Goldberg, D, Wuite, J & Nagler, T 2020, 'Repeat Subglacial Lake Drainage and Filling beneath Thwaites Glacier', *Geophysical Research Letters*. <https://doi.org/10.1029/2020GL089658>

Digital Object Identifier (DOI):

[10.1029/2020GL089658](https://doi.org/10.1029/2020GL089658)

Link:

[Link to publication record in Edinburgh Research Explorer](#)

Document Version:

Peer reviewed version

Published In:

Geophysical Research Letters

Publisher Rights Statement:

This article is protected by copyright. All rights reserved.

General rights

Copyright for the publications made accessible via the Edinburgh Research Explorer is retained by the author(s) and / or other copyright owners and it is a condition of accessing these publications that users recognise and abide by the legal requirements associated with these rights.

Take down policy

The University of Edinburgh has made every reasonable effort to ensure that Edinburgh Research Explorer content complies with UK legislation. If you believe that the public display of this file breaches copyright please contact openaccess@ed.ac.uk providing details, and we will remove access to the work immediately and investigate your claim.



1 **Repeat Subglacial Lake Drainage and Filling beneath Thwaites Glacier**

2 **G. Malczyk¹, N. Gourmelen¹, D. Goldberg¹, J. Wuite², and T. Nagler²**

3 ¹School of Geosciences, University of Edinburgh, Edinburgh, UK.

4 ²ENVEO IT GmbH, Innsbruck, Austria.

5 Corresponding author: George Malczyk (G.R.Malczyk@sms.ed.ac.uk)

6 **Key Points:**

- 7 • Evidence of a drainage event at the lake region of the Thwaites glacier during 2017, four
8 years after previous activity.
- 9 • Contrasting lake behaviors, drainage volume, discharge, and timing of events between the
10 2013 and 2017 events.
- 11 • Observations of recharge rates suggest that modelled melt water production is
12 underestimated.
13

14 **Abstract**

15 Active subglacial lakes have been identified throughout Antarctica, offering a window into
16 subglacial environments and their impact on ice sheet mass balance. Here we use high-resolution
17 altimetry measurements from 2010 to 2019 to show that a lake system under the Thwaites glacier
18 undertook a large episode of activity in 2017, only four years after the system underwent a
19 substantial drainage event. Our observations suggest significant modifications of the drainage
20 system between the two events, with 2017 experiencing greater upstream discharge, faster lake-
21 to-lake connectivity, and the transfer of water within a closed system. Measured rates of lake
22 recharge during the inter-drainage period are 137% larger than modelled estimates, suggesting
23 processes that drive subglacial meltwater production, such as geothermal heat flux or basal
24 friction, are currently underestimated.

25

26 **Plain Language Summary**

27 Antarctic subglacial lakes can play an important role in ice sheet dynamics. When subglacial
28 lakes drain, they release large amounts of water that interact with the subglacial drainage system.
29 Here we show lakes draining only four years after a previous drainage event. Our results suggest
30 that lake activity increases the efficiency of the subglacial drainage network. Rates of lake
31 recharge indicate that basal melt-water production is significantly higher than previously
32 thought.

33 **1. Introduction**

34 The vast majority of ice in the Antarctic ice sheet drains from the continent to the ocean through
35 fast-flowing ice streams and glaciers (Rignot et al., 2011). The presence of meltwater at the bed
36 reduces basal stress, allowing the ice masses to sustain high velocities in some regions (Alley et
37 al., 1986; Kamb, 2001). The movement of water has also been linked to transient glacier flow
38 acceleration (Stearns et al., 2008) and to enhanced melt at the grounding line (Le Brocq et al.,
39 2013; Wei et al., 2020). Therefore, the presence, location, and movement of water at the ice-bed
40 interface are likely significant controls on the mass balance of Antarctica (Bell, 2008). The
41 transport of water from upstream regions to downstream zones was once thought to be a steady-
42 state process (Parizek et al., 2002); however, satellite observations indicate that the movement of
43 subglacial water might be episodic (Gray *et al.*, 2005; Wingham *et al.*, 2006). Observations of
44 localized height anomalies have been interpreted as subglacial water moving in and out of
45 subglacial lakes causing a response at the surface of the glacier. Subglacial lakes located within
46 the interior of the ice sheet are thought to be in a steady state with only localized impact on ice
47 flow (Siegert et al., 2005), whilst lakes located in fast-flowing regions could temporarily alter
48 Antarctic mass balance by modulating the amount and location of subglacial water through
49 episodic drainage events (Siegfried et al., 2018).

50 Active subglacial lakes have been identified throughout Antarctica with satellite altimetry and
51 ice-penetrating radar (Smith et al., 2009; Wright and Siegert, 2012). Observations of surface
52 elevation changes indicate that subglacial lakes are hydraulically connected (Fricker & Scambos,
53 2009; Wingham et al., 2006), and often exist in groups beneath Antarctic ice streams. During the
54 ICESat-1 mission, operating from 2003 to 2010, no subglacial lakes were observed under the
55 Amundsen Sea Sector of the Antarctic Ice Sheet, which was attributed to inadequate
56 measurements due to cloudy conditions (Smith et al., 2017). Analysis of ice-penetrating radar

57 identified a region of high specularity under the Thwaites glacier, interpreted as evidence of the
58 presence of water in distributed channels at the base of the ice sheet (Schroeder et al., 2013). In
59 2017, four large connected active subglacial lakes were discovered under the Thwaites Glacier
60 from analysis of swath processed CryoSat-2 data, which indicated that the lakes drained
61 simultaneously between June 2013 and January 2014 (Smith et al., 2017). Examination of the
62 modelled subglacial melt production in the region suggested that the lakes should have a refill
63 and drainage recurrence interval between 5 and 83 years, depending on whether the recharge
64 scenario involved local melt production only, or melt generated across the larger upstream
65 catchments.

66 Here we use CryoSat-2 altimetry to produce elevation time series which extends the record of
67 lake activity to mid-2019 and describes a second drainage event in 2017. The occurrence of two
68 drainage events within a short timeframe allow us to explore the impact of drainage activity on
69 the evolution of the subglacial system, and to quantify sub-glacial melt supply providing rare
70 insights into sub-glacial processes and basal melt generation.

71 **2. Data and Methods**

72 *2.1 Surface elevation and volume change estimates*

73 Time-dependent elevations were generated using swath processing of CryoSat-2 level L1b
74 SARin data acquired between 2010 and 2019. In contrast to the commonly used point of closest
75 approach (POCA), swath processed SARin exploits the full radar waveform to resolve
76 substantially more elevation than that of the POCA (Gourmelen et al., 2018; Gray et al., 2013;
77 Hawley et al., 2009).

78 To determine the spatial behavior of subglacial lake activity, average rates of surface elevation
79 change were computed using a plane-fitting algorithm (McMillan et al., 2014) applied to swath
80 processed SARin data from late-2014 to mid-2019. Due to the dense elevation field provided by
81 swath processing our region was gridded at a 500-meter posting, with each cell incorporating a
82 search radius of 1.5 km to lower map noise. Within each pixel time-dependent elevations were
83 obtained by fitting a weighted hyperplane against easting, northing, and time; with a time-
84 dependent coefficient retrieved from the regression representing the linear rate of surface change
85 (Foresta et al., 2016). The model was fitted iteratively to the data, omitting elevations differing
86 more than three standard deviations away from the model fit until no further outliers were
87 detected. These maps were used to create masks encapsulating lake activity, which we define as
88 a region with significant localized elevation change ($> 0.5 \text{ m yr}^{-1}$) relative to the background
89 signal (Fricker *et al.*, 2007; Flament, Berthier and Rémy, 2014; Smith *et al.*, 2017).

90 The temporal behavior of the lake system was determined through the creation of a surface
91 elevation change timeseries between 2010 and 2019. We used an adapted version of the point-to-
92 point method (see Text S1 for a detailed description) outlined in Gray *et al.*, (2015) and Gray *et*
93 *al.*, (2019) over our lake outlines to determine time-dependent elevations at a 45-day resolution,
94 with elevations averaged over a 45-day search radius. To isolate the behavior of each lake
95 relative to the catchment we removed the background thinning signal. This was achieved by

96 deducing time-dependent elevations, as per the method above, using a 5 km exclusion area
97 around each lake and subtracting it from the lake's signal.

98 Note that, although the input dataset is similar, both the spatial and temporal approach followed
99 here should lead to slightly different spatio-temporal smoothing compared against previous
100 estimates of 2013 activity. (Smith et al., 2017; see Text S2).

101 Volume change through time was derived by integrating elevation change against the area of
102 each lake mask. For any time-dependent volume change, an approximate statistical error is given
103 by the average of the standard deviations divided by the square root of the number of timeseries
104 realizations. Our volume estimates typically have a standard error of $\pm 0.02 \text{ km}^3$. This is a lower
105 bound on our uncertainty, as the method of spatial and temporal sampling are likely to introduce
106 additional uncertainty. In the absence of an alternative approach, we approximate the volume
107 budget of subglacial water flux by the volume corresponding to the surface deflation, although
108 we acknowledge that this assumption leads to additional uncertainty (Smith et al., 2017,
109 Sergienko et al., 2007). Recharge rates were calculated by applying linear regression against
110 volume change and time during the inter-drainage period, with the resulting rate representing the
111 annual water supply to each lake. Our recharge rates have an uncertainty range derived by
112 calculating a 95% confidence interval with the standard error of regression slope. These rates
113 were compared against modelled local and total melt supplies (Table 1 in Smith et al., 2017).

114 *2.2 Hydraulic potential mapping and estimating subglacial water flow*

115 To identify likely subglacial flow routes, and therefore determine the possible location of
116 subglacial channels, we mapped hydraulic potential (see Text S3), forced using BedMachine ice
117 thickness and bed elevation data, assuming water pressure everywhere at overburden
118 (Morlighem, 2019). Closed depressions within our hydropotential map were filled to represent
119 the large-scale basal flow pattern, as discussed by Smith *et al.*, (2017). We applied a D8 routing
120 scheme to our edited hydropotential grid to calculate the predicted motion of water throughout
121 the glacier bed (Schwanghart & Scherler, 2014).

122 To gauge whether changing lake height might have an impact on the hydraulic gradients which
123 drive water transport, background hydraulic gradients between the lakes were calculated by
124 averaging hydraulic pressure change within each lake mask normalized by the distance between
125 lakes. This was calculated from a hydraulic potential map without depressions filled. The
126 background gradients represent potential gradients between each lake calculated from bed
127 topography and ice thickness alone. During the drainage events, basal water pressure was
128 assumed equal to ice overburden pressure and we estimated the change in potential gradients
129 between the lakes by normalizing the change in lake height against distance along predicted flow
130 routes. It is worth noting that as the lakes water level rises or drops, basal water pressure is likely
131 to exceed or be less than overburden, which could introduce additional uncertainty to our change
132 in gradients.

133 We allowed for the possibility that subglacial melt generated by dissipation in the subglacial
134 network could contribute to the basal water budget. An assumption of Röthlisberger (R-)

135 channels was made, allowing for calculation of channel characteristics and melt production
136 (Schoof, 2010), forced with average discharge rates (see Text S4).

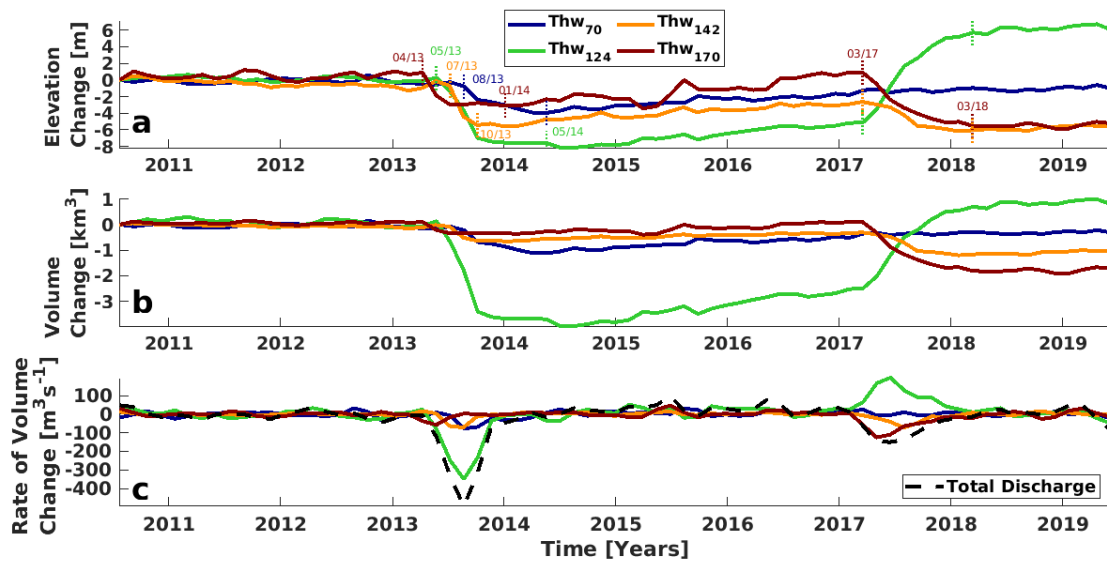
137 *2.3 Divergence mapping*

138 A divergence map was derived to determine the impact of ice flow divergence on surface
139 elevation change during the inter-drainage period. Monthly mean ice surface velocity maps of
140 Thwaites glacier, gridded at 200m, were derived from 6 and 12 day repeat pass Sentinel-1A and
141 -1B Synthetic Aperture Radar (SAR) data acquired in Interferometric Wide (IW) swath mode
142 using offset tracking (Nagler *et al.*, 2015). We created a velocity composite from January 2014 to
143 March 2017 by averaging the monthly velocity maps over the same period. Maps with less than
144 50% coverage of the lake region were omitted from this calculation. A divergence map was
145 produced according to Alley *et al.* (2018), forced using our velocity composite and BedMachine
146 ice thickness data from October 2018 (Morlighem, 2019). The length scale used to produce the
147 maps is adaptive and based upon ice thickness multiplied by a factor of eight.

148 **3. Results**

149 *3.1 2013 and 2017 lake drainage activities*

150 Our timeseries of surface elevation change over the Thwaites subglacial lake system (Figure 1)
151 captures the 2013 activity discussed by Smith *et al.*, (2017) and indicates that lake activity
152 commenced in succession. It appears that the most upstream lake, Thw₁₇₀, was first to activate in
153 early April 2013, draining until early January 2014 with a total volume loss of $0.45 \pm 0.03 \text{ km}^3$.
154 Second in the procession was Thw₁₂₄, draining from mid-May 2013 until May 2014 with a total
155 water loss of $3.83 \pm 0.11 \text{ km}^3$. Thw₁₄₂ activated from early July 2013 draining until October 2013
156 with an average volume loss of $0.55 \pm 0.03 \text{ km}^3$. Last in succession was Thw₇₀ which drained
157 from mid-August 2013 until May 2014 with a total water loss of $0.90 \pm 0.06 \text{ km}^3$. Note that this
158 succession is nearly identical to the one proposed by Smith *et al.*, (2017) except for Thw₁₂₄,
159 which we find to drain later in the sequence. This disagreement is attributed to the temporal
160 smoothing effect of the solution proposed by Smith *et al.*, (2017). We observe a second episode
161 of lake activity upstream of Thw₇₀ from early-2017, indicating a previously unobserved episode
162 of lake drainage. Thw₁₄₂ and Thw₁₇₀ deflated from mid-March 2017 until mid-March 2018, with
163 a total volume loss of $0.89 \pm 0.05 \text{ km}^3$ and $1.91 \pm 0.06 \text{ km}^3$ respectively, draining significantly
164 more water than during 2013 activity. Over the same period Thw₁₂₄ inflated by $3.20 \pm 0.06 \text{ km}^3$
165 and settled 5.2 meters higher than prior to 2013 drainage. Thw₇₀ shows no evidence of either
166 drainage or recharge during 2017, remaining at a near-constant elevation.



167

168 **Figure 1.** Mean elevation and volume change of subglacial lakes relative to July 2010. Elevation and volume changes from 2010
 169 until 2017 were derived assuming 2013 lake sizes, whilst 2017 to 2020 changes were derived using 2017 lake sizes. Vertical
 170 dashed lines represent the onset and termination of lake activity. (a) Mean elevation change within feature boundaries. (b) Mean
 171 volume change within feature boundaries. (c) Derivative of volume change for each lake. Black dashed line represents total
 172 discharge within the subglacial system.

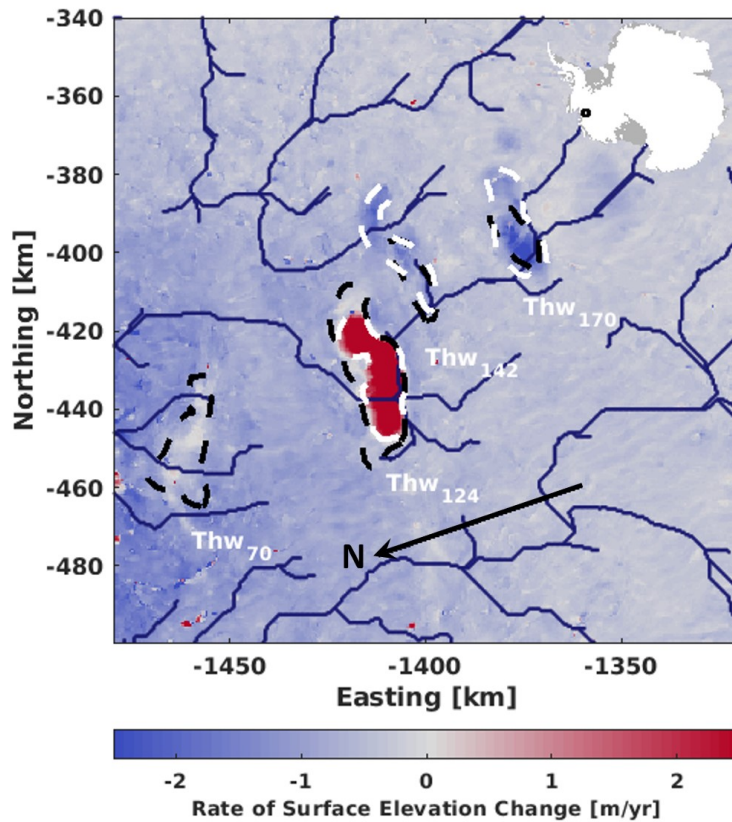
173

3.2 Increase in lake area

174

During the 2017 drainage event the upstream lakes change sized compared against the extent of
 175 activity in 2013 (Figure 2). Thw₁₇₀ and Thw₁₄₂ lake area expanded by 55 km² and 64 km²

176 respectively, both to the east of the 2013 boundaries. Thw₁₂₄ area decreased by 120 km² during
 177 2017 activity, whilst maintaining the general shape of the 2013 boundary.



178
 179 **Figure 2.** Rates of surface elevation change for the Thwaites lake region from January 2014 to August 2019. Location of the lake
 180 region is illustrated by the map insert. Black dashed lines represent lake boundaries during the 2013 event as described in Smith
 181 *et al.*, (2017). White dashed lines represent lake boundaries during the 2017 drainage event. Navy lines represent theoretical
 182 drainage routes derived by applying a D8 routing algorithm to a hydro-potential map of the region.

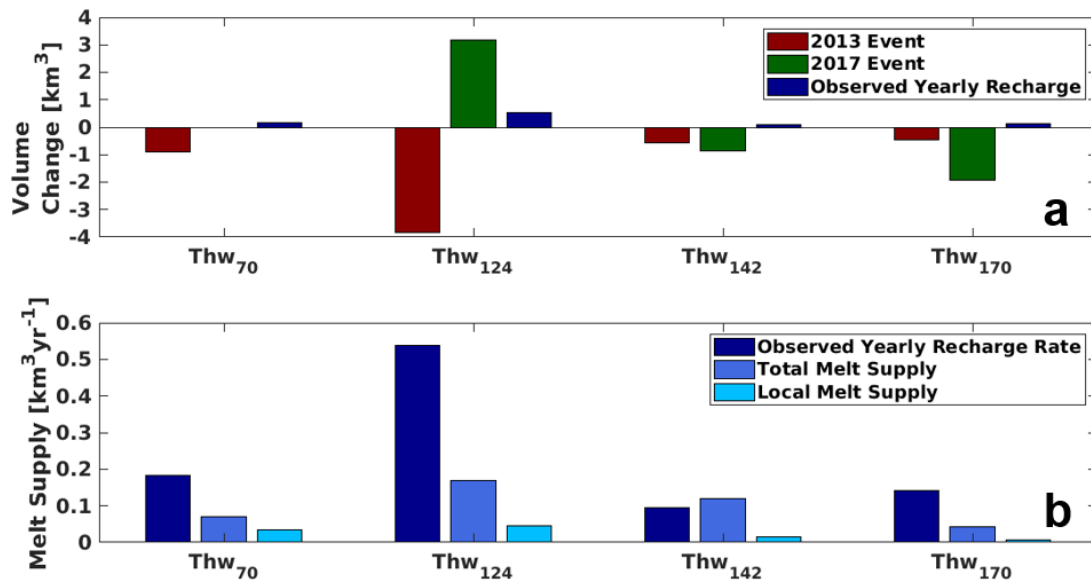
183 3.3 Recharge period

184 Following the termination of lake activity in 2014, the lakes steadily regained volume over the
 185 inter-drainage period. Thw₇₀, Thw₁₂₄, Thw₁₄₂, and Thw₁₇₀ gained 0.90 ± 0.06 , 1.44 ± 0.11 , $0.29 \pm$
 186 0.03 , and 0.46 ± 0.03 km³ over 5.1, 2.6, 3.3, and 3.1 years respectively. Notably, by mid-2017,
 187 Thw₁₇₀ regained the elevation that was lost during the 2013 drainage event, whilst elevation for
 188 the other lakes increased but remained below pre-2013 levels. We believe that this volume gain
 189 was predominantly caused by recharge through subglacial water transport, rather than ice flow
 190 divergence or blowing snow. Divergence has a negligible role, as our observations suggest an
 191 impact of no more than 0.1 m yr^{-1} (see Figure S1). If blowing snow had an impact, we would
 192 expect a bias in elevation change towards the prevailing wind direction – a result that we do not
 193 observe (see Figures S2 and S3). These volume changes correspond to a yearly recharge rate of
 194 0.18 ± 0.02 , 0.57 ± 0.05 , 0.10 ± 0.01 and 0.14 ± 0.03 km³ yr⁻¹ at Thw₇₀, Thw₁₂₄, Thw₁₄₂, and
 195 Thw₁₇₀ respectively. It is worth noting these rates potentially reflect the balance between positive

196 contributions from sub-glacial melt production and leakage from upstream lakes, and negative
197 contribution from leakage of the lakes into the downstream system.

198 3.4 Water Budget

199 Our observations of volume change for 2017 (Figure 3) can be used to determine the behavior of
200 the subglacial drainage system during the drainage activity. Both the 2013 and 2017 drainage
201 events, as well as the predicted drainage pathway (Figure 2), demonstrate the connectivity of the
202 lake system. We assume that all discharged water from the two upstream lakes directly
203 contributes to the rapid recharge of Thw₁₂₄. A total of 2.80 km³ of water from the two upstream
204 lakes contributed to fill Thw₁₂₄, accounting for 87.5% of the observed volume gain. The
205 inclusion of Thw₁₂₄'s recharge rate in the budget leads to a predicted volume gain of 3.37 km³:
206 0.17 km³ larger than the observed increase of 3.20 km³. This excess water falls within the
207 uncertainty range attached to our volume change estimates, which suggests that the filling at
208 Thw₁₂₄ is a product of the drainage of the two upstream lakes and background melt production.



209 **Figure 3.** Volume change and melt supply to each subglacial lake. (a) Mean volume change for the 2013 and 2017 drainage
210 events and estimated yearly recharge rates. Recharge rates represents average yearly volume change for each lake. (b) Different
211 values of potential melt supply to each feature. Local (within basin) and total (within basin and upstream) melt supply obtained
212 from smith et al., (2017).
213

214

215 As the lakes are connected sub-glacially, any change to water levels impacts the hydraulic
216 gradients between the lakes. Background hydraulic gradients from Thw₁₇₀ to Thw₁₄₂, Thw₁₇₀ to
217 Thw₁₂₄, and Thw₁₄₂ to Thw₁₂₄ are 7.72×10^{-3} , 7.64×10^{-3} , and 7.83×10^{-3} respectively. During
218 2017 activity hydraulic gradients from Thw₁₇₀ to Thw₁₄₂, Thw₁₇₀ to Thw₁₂₄ and Thw₁₄₂ to Thw₁₂₄
219 decreased by 1.58×10^{-4} , 5.18×10^{-4} , and 1.60×10^{-3} accordingly. This represents an approximate
220 20% decrease in potential gradients against the background hydraulic gradient (see Figure S4).

221

222

3.5 Subglacial Water Flow

223 During 2013 activity Thw₁₂₄, Thw₁₄₂, and Thw₁₇₀ displayed dynamic volume change over 240,
224 180, and 150 days respectively, whilst in 2017 each lake was active for approximately 300 days
225 (Figure 1). Water fluxes also show contrasting behavior between the 2013 and 2017 events. In
226 2013 the rate of volume change was roughly symmetrical on either side of the peak discharge,
227 whilst 2017 displays clear asymmetry – with post-peak discharge spanning three times the
228 duration of pre-peak discharge.

229 Peak discharge reached 495.8 m³ s⁻¹ in 2013, with an average discharge of 141.7 m³ s⁻¹ and 84.4
230 m³ s⁻¹ for 2013 and 2017 respectively. For individual lakes, average 2013 discharge was 34.4,
231 110.3, 49.3, and 16.2 m³ s⁻¹ for Thw₇₀, Thw₁₂₄, Thw₁₄₂, and Thw₁₇₀ respectively. Average 2017
232 discharge for Thw₁₄₂ and Thw₁₇₀ was 33.8 and 50.6 m³ s⁻¹ respectively, considerably larger
233 during this event than the previous. Thw₁₂₄ gains volume at an average rate of 118.6 m³ s⁻¹.

234

235 Using a simple R-channel assumption for modelling drainage pathways between the lakes, we
236 found that average discharge rates from Thw₁₇₀ during 2017 activity lead to a channel with cross-
237 sectional area of 14.6 m² and a radius of 3.0 m. Water within this channel would flow at a mean
238 velocity of 3.5 m s⁻¹, causing melt at the channels side walls at a rate of 0.25 m³ s⁻¹. Assuming
239 this melting rate was sustained over the period of lake activity an additional 0.008 km³ of water
240 would be injected into the subglacial system – negligible compared against the water mobilized
241 from the lakes. Should channel behavior be dictated by the combined discharge from Thw₁₇₀ and
242 Thw₁₄₂ we would expect a channel with a cross-sectional area of 22.1 m² and radius of 3.8 m.
243 Water would flow at a mean velocity of 3.8 m s⁻¹, which corresponds to a melting rate of 0.42 m³
244 s⁻¹. A channel of this size would contribute 0.013 km³ of water to the subglacial system during
245 2017 activity.

246 **4 Discussion**

247 *4.1 Water Budget*

248 The net volume change of the ice sheet must be conserved from principles of mass conservation.
249 Therefore, observing the flux of each lake allows us to infer the movement of water throughout
250 the subglacial system. Thw₁₂₄ appears to be the downstream limit of the drainage event in 2017.
251 Hence, we assume that water discharged from upstream lakes combined with Thw₁₂₄ recharge
252 rate and drainage-related melting of the channels side was responsible for the observed volume
253 gain. Under this assumption we expect to see a volume gain of 3.37 km³, which is 0.17 km³
254 greater than the actual volume gain observed at Thw₁₂₄ - but falls within the uncertainty range.
255 Background recharge rates are required to close the water budget, as without this component the
256 water supply into Thw₁₂₄ would be too low to explain the observed volume gain. Unlike in 2013,
257 where the four lakes drained out of the system, there is no evidence of subglacial lake activity
258 downstream of Thw₁₂₄ in 2017 (Figure 1).

259 *4.2 Notable differences in behavior between drainage events*

260 Our observations highlight a marked difference in the rate and evolution of water movement
261 between lakes during the 2013 and 2017 events. First: during the 2013 drainage event lake
262 activity followed a cascading pattern spanning six months, whilst in 2017 all lakes activated
263 nearly simultaneously (Figure 1). Second: volume change, average and peak discharge at Thw₁₇₀
264 were significantly larger in 2017, being 324%, 212%, and 89% respectively above that of the

265 2013 activity. Third: Thw_{170} drained at a similar elevation in 2013 and 2017, whilst Thw_{142}
266 drained below its 2013 level and Thw_{124} exceeded 2013 levels in 2017 without triggering
267 drainage. Fourth: both Thw_{142} and Thw_{170} settled at a lower elevation in 2017 relative to 2013
268 (Figure 1a), suggesting the upstream lakes only experienced partial drainage in 2013.

269 Despite the apparent simultaneous activity in 2017, we suspect the lakes activity followed a
270 cascading pattern, similar to what occurred in 2013, but with a significantly faster transfer of
271 water that our timeseries temporal resolution could not resolve. In such a scenario, Thw_{170} would
272 activate first and trigger Thw_{142} , with discharged water filling Thw_{124} . This scenario is further
273 evident considering that Thw_{170} drained at similar volumes in 2013 and 2017, which suggests the
274 lake overcame its hydro-potential barrier during both drainage events. Therefore, Thw_{170} could
275 be considered the trigger to lake activity within the system and might be responsible for
276 controlling future drainage events.

277 The rapid transfer of water in 2017 might have been made possible due to the development of a
278 more efficient drainage system, likely following 2013 activity. Several possible mechanisms
279 could be responsible for this change. For instance, discharge rates from the 2013 drainage event
280 might have caused the formation of a channelized system between the lakes. While such
281 channels would likely shrink due to creep closure, they may not have fully closed due to the
282 transfer of water between the lakes during the inter-drainage period. This could precondition the
283 system, allowing for rapid channel expansion during 2017 activity. Alternatively, discharge from
284 the 2013 event might have caused sediment mobilization and potential channel erosion, leading
285 the development of a more efficient drainage system (Brisbourne et al., 2017; Kirkham et al.,
286 2019). Our reasoning is speculative as there is insufficient evidence available to either validate or
287 negate these hypotheses. Nevertheless, this change in efficiency indicates complex behavior of
288 the subglacial system, which is deserving of further study.

289 Discharge rates displayed a clear symmetrical ramp up and descent pattern in 2013 (Figure 1c).
290 Conversely, discharge rates in 2017 spiked rapidly before tailing off over six months. All lakes
291 drained in 2013 indicating an open system, whilst in 2017 the subglacial system could be
292 considered closed, with a limit at Thw_{124} which collected water and prevented significant
293 discharge downstream. The influx of water into Thw_{124} would have increased the pressure head
294 within the lake, while the pressure head of upstream features was decreased due to the lower
295 water levels. Potential gradients between the features decreased by 20%, which might have been
296 sufficient to prolong the discharge of upstream water. Hence, the prolonged tail of discharge
297 rates in 2017.

298 *4.3 Observations regarding Thw_{124}*

299 The conditions and triggers of lake drainage are still poorly understood. While Thw_{170} likely
300 acted as a trigger for both 2013 and 2017 events, Thw_{124} displayed contrasting behavior. Thw_{124}
301 drained in 2013 but not in 2017, despite larger upstream discharge and the fact that the lake
302 water level, following termination of 2017 activity, exceeded that of pre-2013 drainage (Figure
303 1). This suggests that Thw_{124} could be acting like a roadblock, collecting water whilst preventing
304 significant discharge downstream. The shut-down of downstream drainage could have taken
305 place as early as mid-2014 during the onset of lake refill (Figure 1), in particular because Thw_{124}
306 refill took place at a rate three-fold higher than at any of the other lakes (Figure 3) and that

307 modelling does not predict such a significant difference in refill rates between lakes (Smith et al.,
308 2017).

309 The mechanism behind the change in behavior of Thw_{124} is uncertain. As hypothesized earlier,
310 the significant discharge rates from 2013 activity might have modified the hydraulic properties
311 of the system, which might have formed a barrier to flow downstream. Alternatively, it could be
312 related to the mode of channel formation. Recent modelling suggests that the accumulation of
313 water within lake basins steepens the hydraulic gradient and allows greater flux downstream,
314 which melts channels that can trigger drainage (Dow et al., 2016, Dow et al., 2018). Prior to
315 2013 activity Thw_{124} appeared to be at hydrostatic equilibrium, whereby flow into the lake is
316 equal to flow out, evident by the sustained overall lake volume (Figure 1). This outwards flow
317 might have melted small channels immediately downstream of the lake. During 2013 activity,
318 when water from upstream reached Thw_{124} , hydraulic gradients would steepen. This would force
319 water over the downwards slope, melting larger channels and likely triggering drainage. As the
320 drainage event tails off, discharge rates decrease causing creep closure within the channels.
321 During the inter-drainage period, the behavior of the system changes which limits the amount of
322 water discharged from Thw_{124} , which would hamper the creation of channels. The influx of
323 water from the 2017 event would increase hydropotential gradients between the lake and
324 downstream, driving water over the reverse slope. However, inefficient downstream channels
325 might have prevented drainage.

326 *4.4 Recharge rates*

327 Our annual recharge rates are significantly above estimations based on simulations of melt
328 generation and water routing, whether considering melt production over local or regional
329 catchments (Smith et al., 2017). There is a degree of variability between lakes, with rates at
330 Thw_{70} , Thw_{124} , and Thw_{170} significantly above predicated recharge, whilst Thw_{142} is close to the
331 high-end estimate of Smith et al., (2017) (Figure 3b). The variability between predicted and
332 observed recharge rates can be explained by lake-to-lake water transfer, along with uncertainty in
333 the subglacial network. However, the overall discrepancy between our observed rates and
334 modelled values suggest estimates of melting rates at the bed are likely substantially
335 underestimated. It is likely modelled subglacial melt production was underestimated, at least in
336 part, because modelled melt did not incorporate the elevated geothermal heat flux that has been
337 suggested based on radar observations located within the Thwaites lakes' catchments (Schroeder
338 et al., 2014). In particular, Schroeder et al., (2014) suggests there may localized hot spots where
339 heat flux is greater than the background. Alternatively, the catchment and water routing used in
340 Smith et al., (2017) may not be representative of the true conditions at the bed, impacting the
341 accuracy of their derived recharge rates. Our altimetrically derived recharge rates seemingly
342 imply the second scenario of Smith et al., (2017): whereby lakes regain discharged water using
343 within catchment-scale melt production and water supplied from upstream. Assuming Thw_{70} ,
344 Thw_{142} , and Thw_{170} recharge at the same rate as per the inter-drainage period we expect each
345 lake to regain its pre-2013 levels in 3.2, 11.5, and 13.6 years respectively. Estimates derived
346 from modelled total melt production instead imply a recharge time of 8.1, 9.6, and 43.4 years for
347 Thw_{70} , Thw_{142} and Thw_{170} respectively. Given Thw_{170} likely triggered the 2013 and 2017

348 drainage events, and will likely trigger future events, the significantly shorter recharge time
349 implies the drainage cycle of the system is shorter than previously thought.

350 **5 Conclusions**

351 In mid-2013 a system of interconnected subglacial lakes under the central part of the Thwaites
352 glacier drained (Smith et al., 2017). Our altimetry measurements reveal a second period of lake
353 activity in 2017, with discharged water tracked throughout the system. Both events are
354 compatible with a cascading transfer of water, initiated by the most upstream lake. Observations
355 reveal significant differences between the 2013 and 2017 drainage events. Unlike 2013 activity,
356 in 2017 a downstream lake acts as a limit for the movement of subglacial water. This lake
357 displayed rapid recharge, forced with discharge from the upstream lakes, increased in volume by
358 3.20 km³ and settled 5.2 m higher than pre-2013 levels. Across the lake system, discharge is 29%
359 greater in 2017 than in 2013 with lake sizes expanding by 119 km². During 2013 activity each
360 lake initiated within a six-month period, whilst in 2017 the lakes activated within 45-days of
361 each other. These characteristics point towards an increase in efficiency of the active subglacial
362 system in 2017. Observations during the inter-drainage period indicate that lake recharge rates
363 are 137% higher than modelled estimates. This implies that subglacial lakes recharge using melt
364 supplied from local and upstream sources, and that geothermal heat flux and basal friction
365 produce more melt water than currently predicted.

366 **Acknowledgements**

367 This work was performed at the University of Edinburgh under grants from the European Space
368 Agency's project 4DAntarctica (ESA: Grant #4000128611/19/I-DT), and from the PROPHET
369 project, a component of the International Thwaites Glacier Collaboration (ITGC). Support from
370 National Science Foundation (NSF: Grant #1739031) and Natural Environment Research
371 Council (NERC: Grants NE/S006745/1, NE/S006796/1 and NE/T001607/1). ITGC Contribution
372 No. 024. G.R.M. acknowledges a NERC PhD Studentship. The authors wish to thank ESA for
373 providing open access to CryoSat-2 data, and M. Morlighem for open access to Bedmachine.
374 The authors are grateful to the editor, Mathieu Morlighem, and to two anonymous reviewers,
375 whose comments have significantly improved the manuscript.

376 **Data Availability Section**

377 Our rate of change maps, lake masks and lake timeseries are freely available from 4D Antarctica
378 (<https://4d-antarctica.org/products/>). The CryoSat-2 satellite altimetry data are freely available
379 from the European Space Agency (<https://earth.esa.int/web/guest/data-access>). The BedMachine
380 ice thickness and bed elevation data are freely available from the National Snow and Ice Data
381 Centre (<https://nsidc.org/data/NSIDC-0756/versions/1>). The ice velocity products are based on
382 Copernicus Sentinel-1 data made available through the European Space Agency; the products are
383 available upon request (<http://cryoportals.enveo.at>). The wind velocity and direction data are
384 freely available from the Physical Sciences Laboratory
385 (<https://psl.noaa.gov/data/gridded/data.ncep.reanalysis.derived>).

386 **References**

387
388 Alley, K. E., Scambos, T. A., Anderson, R. S., Rajaram, H., Pope, A., & Haran, T. M. (2018).

- 389 Continent-wide estimates of Antarctic strain rates from Landsat 8-derived velocity grids.
390 *Journal of Glaciology*, 64(244), 321–332. <https://doi.org/10.1017/jog.2018.23>
391
- 392 Alley, R. B., Blankenship, D. D., Bentley, C. R., & Rooney, S. T. (1986). Deformation of till
393 beneath ice stream B, West Antarctica. *Nature*, 322(6074), 57–59.
394 <https://doi.org/10.1038/322057a0>
395
- 396 Bartholomaeus, T. C., Anderson, R. S., & Anderson, S. P. (2008). Response of glacier basal
397 motion to transient water storage. *Nature Geoscience*, 1(1), 33–37.
398 <https://doi.org/10.1038/ngeo.2007.52>
399
- 400 Bell, R. E. (2008, May). The role of subglacial water in ice-sheet mass balance. *Nature*
401 *Geoscience*. Nature Publishing Group. <https://doi.org/10.1038/ngeo186>
402
- 403 Smith, B., Fricker, H., Joughin, I., & Tulaczyk, S. (2009). An inventory of active subglacial
404 lakes in Antarctica detected by ICESat (2003–2008). *Journal of Glaciology*, 55(192), 573–
405 595. <https://doi.org/10.3189/002214309789470879>
406
- 407 Björnsson, H. (1992). Jokulhlaups in Iceland: prediction, characteristics and simulation. *Annals*
408 *of Glaciology*, 16, 95–106. <https://doi.org/10.3189/1992aog16-1-95-106>
409
- 410 Björnsson, H. (2002). Subglacial lakes and jökulhlaups in Iceland. *Global and Planetary*
411 *Change*, 35(3), 255–271. [https://doi.org/10.1016/S0921-8181\(02\)00130-3](https://doi.org/10.1016/S0921-8181(02)00130-3)
412
- 413 Brisbourne, A. M., Smith, A. M., Vaughan, D. G., King, E. C., Davies, D., Bingham, R. G., et al.
414 (2017). Bed conditions of Pine Island Glacier, West Antarctica. *Journal of Geophysical*
415 *Research: Earth Surface*, 122(1), 419–433. <https://doi.org/10.1002/2016JF004033>
416
- 417 Le Brocq, A. M., Ross, N., Griggs, J. A., Bingham, R. G., Corr, H. F. J., Ferraccioli, F., et al.
418 (2013). Evidence from ice shelves for channelized meltwater flow beneath the Antarctic Ice
419 Sheet. *Nature Geoscience*, 6(11), 945–948. <https://doi.org/10.1038/ngeo1977>
420
- 421 Dow, C. F., Werder, M. A., Nowicki, S., & Walker, R. T. (2016). Modeling Antarctic subglacial
422 lake filling and drainage cycles. *The Cryosphere*, 10(4), 1381–1393.
423 <https://doi.org/10.5194/tc-10-1381-2016>
424
- 425 Dow, C. F., Werder, M. A., Babonis, G., Nowicki, S., Walker, R. T., Csatho, B., & Morlighem,
426 M. (2018). Dynamics of Active Subglacial Lakes in Recovery Ice Stream. *Journal of*
427 *Geophysical Research: Earth Surface*, 123(4), 837–850.
428 <https://doi.org/10.1002/2017JF004409>
429
- 430 Flament, T., Berthier, E., & Rémy, F. (2014). Cascading water underneath Wilkes Land, East
431 Antarctic ice sheet, observed using altimetry and digital elevation models. *The Cryosphere*,
432 8(2), 673–687. <https://doi.org/10.5194/tc-8-673-2014>
433
- 434 Foresta, L., Gourmelen, N., Pálsson, F., Nienow, P., Björnsson, H., & Shepherd, A. (2016).

- 435 Surface elevation change and mass balance of Icelandic ice caps derived from swath mode
436 CryoSat-2 altimetry. *Geophysical Research Letters*. <https://doi.org/10.1002/2016GL071485>
437
- 438 Fowler, A. C. (1999). Breaking the seal at Grímsvötn, Iceland. *Journal of Glaciology*, 45(151),
439 506–516. <https://doi.org/https://doi.org/10.3189/S0022143000001362>
440
- 441 Fretwell, P., Pritchard, H. D., Vaughan, D. G., Bamber, J. L., Barrand, N. E., Bell, R., et al.
442 (2012). Bedmap2: improved ice bed, surface and thickness datasets for Antarctica The
443 Cryosphere Discussions Bedmap2: improved ice bed, surface and thickness datasets for
444 Antarctica. *TCD*, 6(6), 4305–4361. <https://doi.org/10.5194/tcd-6-4305-2012>
445
- 446 Fricker, H. A., Carter, S. P., Bell, R. E., & Scambos, T. (2014). Active lakes of recovery ice
447 stream, East Antarctica: A bedrock-controlled subglacial hydrological system. *Journal of*
448 *Glaciology*, 60(223), 1015–1030. <https://doi.org/10.3189/2014JoG14J063>
449
- 450
- 451 Fricker, H. A., & Scambos, T. (2009). Connected subglacial lake activity on lower Mercer and
452 Whillans Ice Streams, West Antarctica, 2003-2008. *Journal of Glaciology*, 55(190), 303–
453 315. <https://doi.org/10.3189/002214309788608813>
454
- 455 Fricker, H. A., Scambos, T., Bindschadler, R., & Padman, L. (2007). An active subglacial water
456 system in West Antarctica mapped from space. *Science*, 315(5818), 1544–1548.
457 <https://doi.org/10.1126/science.1136897>
458
- 459 Gourmelen, N., Escorihuela, M. J., Shepherd, A., Foresta, L., Muir, A., Garcia-Mondéjar, A., et
460 al. (2018). CryoSat-2 swath interferometric altimetry for mapping ice elevation and
461 elevation change. *Advances in Space Research*, 62(6), 1226–1242.
462 <https://doi.org/10.1016/j.asr.2017.11.014>
463
- 464 Gray, L., Burgess, D., Copland, L., Cullen, R., Galin, N., Hawley, R., & Helm, V. (2013).
465 Interferometric swath processing of Cryosat data for glacial ice topography. *Cryosphere*,
466 7(6), 1857–1867. <https://doi.org/10.5194/tc-7-1857-2013>
467
- 468 Gray, L., Burgess, D., Copland, L., Demuth, M. N., Dunse, T., Langley, K., & Schuler, T. V.
469 (2015). CryoSat-2 delivers monthly and inter-annual surface elevation change for Arctic ice
470 caps. *Cryosphere*, 9(5), 1895–1913. <https://doi.org/10.5194/tc-9-1895-2015>
471
- 472 Gray, Laurence. (2005). Evidence for subglacial water transport in the West Antarctic Ice Sheet
473 through three-dimensional satellite radar interferometry. *Geophysical Research Letters*,
474 32(3), L03501. <https://doi.org/10.1029/2004GL021387>
475
- 476 Gray, Laurence, Burgess, D., Copland, L., Langley, K., Gogineni, P., Paden, J., et al. (2019).
477 Measuring Height Change Around the Periphery of the Greenland Ice Sheet With Radar
478 Altimetry. *Frontiers in Earth Science*, 7. <https://doi.org/10.3389/feart.2019.00146>
479
- 480 Hawley, R. L., Shepherd, A., Cullen, R., Helm, V., & Wingham, D. J. (2009). Ice-sheet

- 481 elevations from across-track processing of airborne interferometric radar altimetry.
482 *Geophysical Research Letters*, 36(22). <https://doi.org/10.1029/2009GL040416>
483
- 484 Joughin, I., Tulaczyk, S., Bamber, J. L., Blankenship, D., Holt, J. W., Scambos, T., & Vaughan,
485 D. G. (2009). Basal conditions for Pine Island and Thwaites Glaciers, West Antarctica,
486 determined using satellite and airborne data. *Journal of Glaciology*, 55(190), 245–257.
487 <https://doi.org/10.3189/002214309788608705>
488
- 489 Kalnay, E.; Kanamitsu, M.; Kistler, R.; Collins, W.; Deaven, D.; Gandin, L.; Iredell, M.; Saha,
490 S.; White, G.; Woollen, J. Zhu, Y.; Chelliah, M.; Ebisuzaki, W.; Higgins, W.; Janowiak, J.;
491 MoK.C., C. Ropelewski, Wang, J.; Leetmaa, A.; Reynolds, R.; Jenne, R. and J. D. (1996).
492 Kalnay_1996_Ncep_Reanalysis.Pdf. *Bulletin of the American Meteorological Society*, 437–
493 471. [https://doi.org/10.1175/1520-0477\(1996\)077<0437:TNYRP>2.0.CO;2](https://doi.org/10.1175/1520-0477(1996)077<0437:TNYRP>2.0.CO;2)
494
495
- 496 Kamb, B. (2001). The West Antarctic Ice Sheet: Behavior and Environment Research Series,
497 Volume 77 (pp. 157–199). <https://doi.org/10.1029/ar077p0157>
498
- 499 Kirkham, J. D., Hogan, K. A., Larter, R. D., Arnold, N. S., Nitsche, F. O., Gолledge, N. R., &
500 Dowdeswell, J. A. (2019). Past water flow beneath Pine Island and Thwaites glaciers, West
501 Antarctica. *The Cryosphere*, 13, 1959–1981. <https://doi.org/10.5194/tc-13-1959-2019>
502
- 503 McMillan, M., Shepherd, A., Sundal, A., Briggs, K., Muir, A., Ridout, A., et al. (2014).
504 Increased ice losses from Antarctica detected by CryoSat-2. *Geophysical Research Letters*.
505 <https://doi.org/10.1002/2014GL060111>
506
- 507 Morlighem, M., Rignot, E., Binder, T., Blankenship, D., Drews, R., Eagles, G., et al. (2020).
508 Deep glacial troughs and stabilizing ridges unveiled beneath the margins of the Antarctic
509 ice sheet. *Nature Geoscience*, 13(2), 132–137. <https://doi.org/10.1038/s41561-019-0510-8>
510
- 511 Nagler, T., Rott, H., Hetzenecker, M., Wuite, J., Potin, P. (2015). The Sentinel-1 Mission: New
512 Opportunities for Ice Sheet Observations. *Remote Sensing*, 7, 9371–9389.
513 <https://doi.org/10.3390/rs70709371>
514
- 515 Parizek, B. R., Alley, R. B., Anandakrishnan, S., & Conway, H. (2002). Sub-catchment melt and
516 long-term stability of ice stream D, West Antarctica. *Geophysical Research Letters*, 29(8),
517 55-1-55-4. <https://doi.org/10.1029/2001gl014326>
518
- 519 Rignot, E., Mouginot, J., & Scheuchl, B. (2011). Ice flow of the antarctic ice sheet. *Science*,
520 333(6048), 1427–1430. <https://doi.org/10.1126/science.1208336>
521
- 522 Schoof, C. (2010). Ice-sheet acceleration driven by melt supply variability. *Nature*, 468(7325),
523 803–806. <https://doi.org/10.1038/nature09618>
524
- 525 Schroeder, D. M., Blankenship, D. D., Young, D. A., & Quartini, E. (2014). Evidence for
526 elevated and spatially variable geothermal flux beneath the West Antarctic Ice Sheet.

- 527 *Proceedings of the National Academy of Sciences of the United States of America*, 111(25),
528 9070–9072. <https://doi.org/10.1073/pnas.1405184111>
529
- 530 Schwanghart, W., & Scherler, D. (2014). Short Communication: TopoToolbox 2-MATLAB-
531 based software for topographic analysis and modeling in Earth surface sciences. *Earth Surf.*
532 *Dynam*, 2, 1–7. <https://doi.org/10.5194/esurf-2-1-2014>
533
- 534 Sergienko, O. V., MacAyeal, D. R., & Bindschadler, R. A. (2007). Causes of sudden, short-term
535 changes in ice-stream surface elevation. *Geophysical Research Letters*, 34(22), L22503.
536 <https://doi.org/10.1029/2007GL031775>
537
- 538 Siegert, M. J., Carter, S., Tabacco, I., Popov, S., & Blankenship, D. D. (2005, September). A
539 revised inventory of Antarctic subglacial lakes. *Antarctic Science*.
540 <https://doi.org/10.1017/S0954102005002889>
541
- 542 Siegfried, M. R., & Fricker, H. A. (2018). Thirteen years of subglacial lake activity in Antarctica
543 from multi-mission satellite altimetry. *Annals of Glaciology*, 59(76pt1), 42–55.
544 <https://doi.org/10.1017/aog.2017.36>
545
- 546 Smith, B. E., Gourmelen, N., Huth, A., & Joughin, I. (2017). Connected subglacial lake drainage
547 beneath Thwaites Glacier, West Antarctica. *Cryosphere*, 11(1), 451–467.
548 <https://doi.org/10.5194/tc-11-451-2017>
549
- 550 Stearns, L. A., Smith, B. E., & Hamilton, G. S. (2008, December 16). Increased flow speed on a
551 large east antarctic outlet glacier caused by subglacial floods. *Nature Geoscience*. Nature
552 Publishing Group. <https://doi.org/10.1038/ngeo356>
553
- 554 Wei, W., Blankenship, D. D., Greenbaum, J. S., Gourmelen, N., Dow, C. F., Richter, T. G., et al.
555 (2020). Getz Ice Shelf melt enhanced by freshwater discharge from beneath the West
556 Antarctic Ice Sheet. *The Cryosphere*, 14(4), 1399–1408. [https://doi.org/10.5194/tc-14-1399-](https://doi.org/10.5194/tc-14-1399-2020)
557 [2020](https://doi.org/10.5194/tc-14-1399-2020)
558
- 559 Wingham, D. J., Siegert, M. J., Shepherd, A., & Muir, A. S. (2006). Rapid discharge connects
560 Antarctic subglacial lakes. *Nature*, 440(7087), 1033–1036.
561 <https://doi.org/10.1038/nature04660>
562
- 563 Wright, A., & Siegert, M. (2012). A fourth inventory of Antarctic subglacial lakes. *Antarctic*
564 *Science*, 24(6), 659–664. <https://doi.org/10.1017/S095410201200048X>
565
566
567